Electronic Supplementary Information for

Thin carbon nanotube coiled around thick branched carbon nanotube composite electrodes for high-performance and flexible supercapacitors

Yongsheng Zhou [*,a,b,c], *Tao Wang* [b], *Shou Peng* [*,a], *Tingting Yao* [a], *Yingchun Zhu* [d,f], *and Bingshe Xu* [e]

[a] State Key Laboratory of Advanced Technology for Float Glass, Bengbu, 233018, P. R. China;

[b] College of Chemistry and Materials Engineering, Anhui Science and Technology University, Bengbu, 233030, P. R. China;

[c] Anhui Province Quartz Sand Purification and Photovoltaic Glass Engineering Research Center, Anhui Science and Technology University, Bengbu, 233000, China;

[d] Key Laboratory of Inorganic Coating Materials CAS, Shanghai Institute of Ceramics, Chinese Academy of Sciences, Shanghai, 200050, P. R. China;

[e] Key Laboratory of Interface Science and Engineering in Advanced Materials, Ministry of Education, Taiyuan University of Technology, Taiyuan, 030024, P. R. China;

[f] Center of Materials Science and Optoelectronics Engineering，University of Chinese Academy of Sciences, Beijing 100049, P. R. China.

E-mail: yszhou1981@gmail.com.

Materials and methods

Synthesis of TCNT/BCNT

Ni/MgO catalyst was synthesized using a typical co-precipitation and subsequent calcination reaction. First, $Ni(NO_3)_2$, and $Mg(NO_3)_2$ were dissolved in 200.0 mL deionized water with $[Ni^{2+}]+[Mg^{2+}]$ = 0.2mol L $^{-1}$. Then, 50 mL 2.5 mol L $^{-1}$ NaOH was added into the solution and the solution was then left to stand at 95 °C for 12 h in a 500 mL flask, which was equipped with a reflux condenser in ambient atmosphere. The as-obtained suspension was filtered, washed by deionized water, and freeze-dried which were then loaded into a quartz boat and then calcined at 600 ^{0}C for 2h in air to decompose the precursor; the resulted powder was then reduced in H_2 (flow rate: 100 sccm) and Ar (flow rate: 300 sccm) for 30 min at 600 ^{0}C to form Ni nanoclusters supported on MgO substrate, which was collected and used as catalyst.

The TCNT/BCNT composites were prepared using a temperature shift two-stage fluidized bed. In detail, 0.2 g Ni/MgO nanoparticles were loaded into the reactor and processed with our customed two-step growth. The first-step growth was held in the upper zone of the reactor with the temperature of 750 °C. C_2H_4 was introduced into the furnace with a flow rate of 100 mL min^{-1}. During the first-step growth, the large-sized catalysts were conceived from the nanoparticles and thick BCNTs were acquired. Then the isolation board was opened and the nanoparticles (with the BCNTs on them) were moved to the lower zone of the reactor with the temperature of 950°C to proceed the second-step growth for another 15 min. During this process, the small catalysts were conceived from the nanoparticles and the thin CNTs (TCNT) were grown on the BCNT. The furnace was cooled to room temperature under Ar protection. The as-grown products were collected and purified by routine HCl (5 mol L^{-1}) and NaOH (13 mol L^{-1}) treatment.

Synthesis of BCNTs

The BCNTs material was synthesized in a similar way in the first-step growth of the TCNT/BCNT composites.

Characterization

Scanning electron microscope (SEM) images were obtained by a Hitachi SEM. The TEM was performed using a JEM-2100 TEM. The crystal phase composition was determined by XRD using a D8 Advance (Bruker) with CuKa radiation. The Raman spectroscopy investigations were performed using a Renishaw inVia Reflex spectrometer with laser wavelength of 532 nm. N_2 sorption analysis was conducted on an ASAP2020 accelerated surface area and porosimetry instrument (Micromeritics), equipped with automated surface area, at 77 K using BarrettEmmettTeller (BET) calculations for the surface area. The pore size distribution (PSD) plot was recorded from the adsorption branch of the isotherm based on the Barrett−Joyner−Halenda (BJH) method. Cyclic voltammetry (CV) tests and galvanostatic charge–discharge (GCD), the electrochemical impedance spectra measurements were carried out by a computer-controlled electrochemical workstation (CHI 760D).

Electrochemical Characterization

The preparation of electrode and analytical measurements of electrochemical properties are described as follows. The as-fabricated TCNT/BCNT composite or BCNTs were pressed into electrode films using standard mold with a pressure of 10 MPa. The electrochemical performances were measured using a two-electrode testing cell using a similar procedure reported in the literature. A glassy fiber filter paper was sandwiched between two electrode films and then infiltrated with corresponding electrolyte solutions, 1.0 M H_2SO_4 and $EMIMBF_4$. Symmetrical flexible supercapacitors were assembled by sandwiching two pieces of TCNT/BCNT electrodes (1.3 × 1.7 cm) and KOH/PVA gel electrolyte between two PET membranes.

The specific capacitance, the energy density (E) and the power density (P) of these cells were calculated using the following equations:

a. the calculation of specific capacitance by CV and GCD curves:

$$C = \frac{\int I dv}{S \bullet \Delta V \bullet m} \quad (1)$$

$$C_s = \frac{I}{m \bullet (dV/dt)} \quad (2)$$

Where I (A) is the discharge current, S (V s^{-1}) is the scan rate, dV/dt is the slope of the discharge curve (V s^{-1}), m (g) is the mass of the single working electrode, and ΔV (V) denotes the voltage change excluding the IR drop during the discharge process.

b. the calculation of energy density (E) and power density (P):

$$E = \frac{C_S \bullet \Delta V^2}{2 \bullet 3.6} \quad (3)$$

$$P = \frac{E \bullet 3600}{\Delta t} \quad (4)$$

Where ΔV (V) denotes the voltage change excluding the IR drop during the discharge process, and Δt (s) is the discharge time.

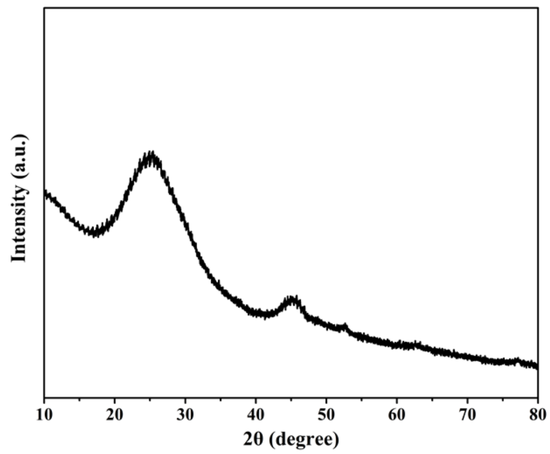

Figure S1. XRD spectroscopic of the TCNT/BCNT.

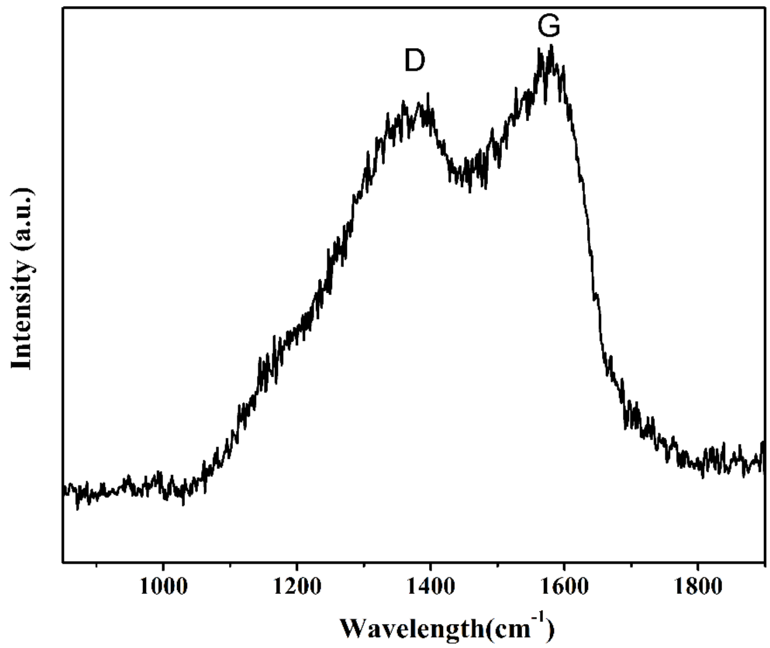

Figure S2. Raman spectroscopic of the TCNT/BCNT.

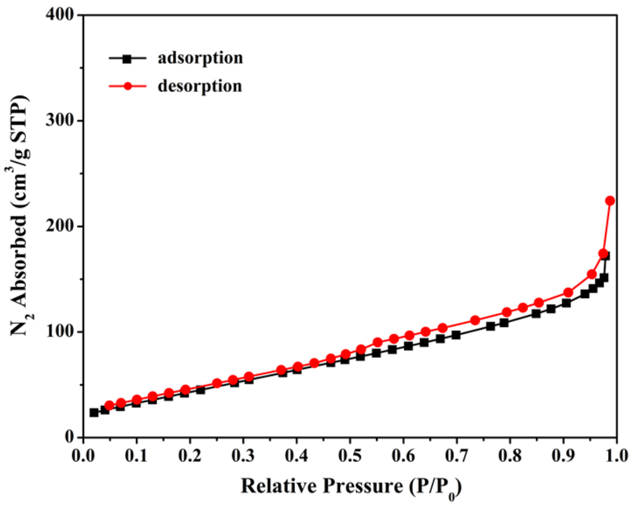

Figure S3. Nitrogen sorption isotherms of BCNT.

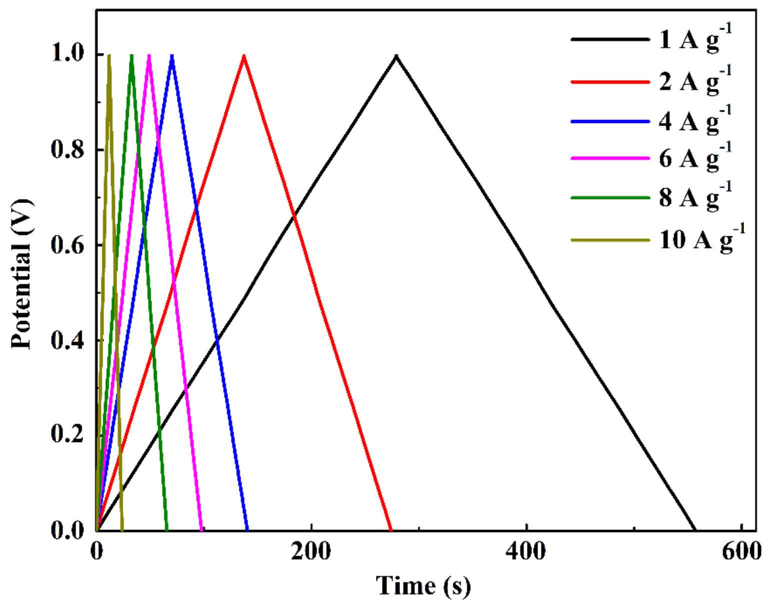

Figure S4. Galvanostatic charge/discharge curves of TCNT/BCNT at different current densities.

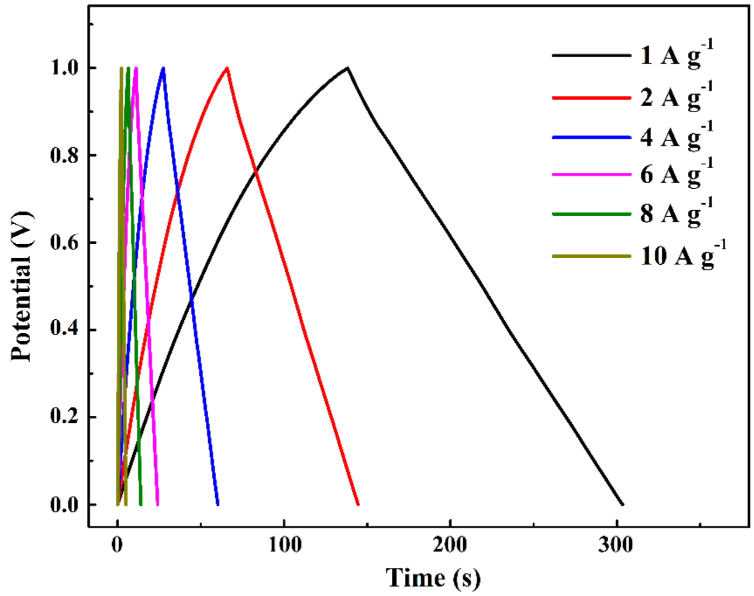

Figure S5. Galvanostatic charge/discharge curves of BCNT at different current densities.

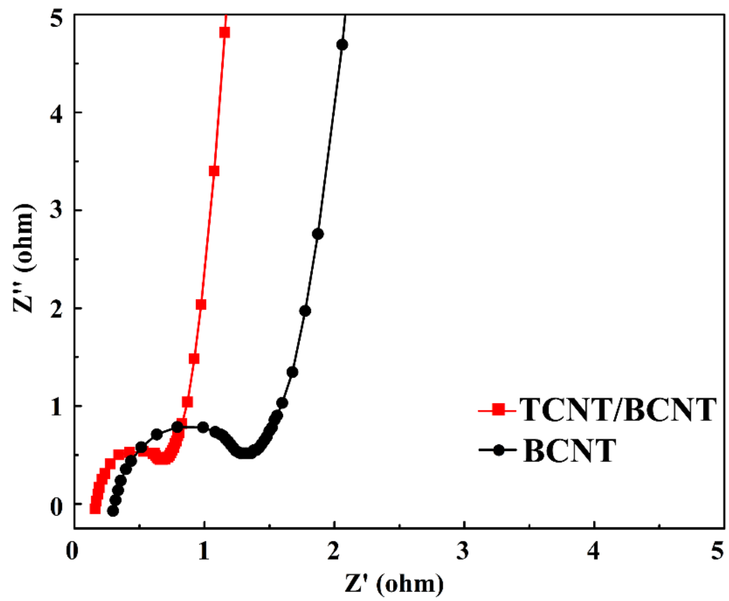

Figure S6. Typical Nyquist plot of the TCNF/BCNT and BCNT.

Table S1| Specific capacitance and energy density values of different CNT-based materials for supercapacitors.

Materials	Capacitance	Energy density	References
NiCo-P/CNT/CW	11.2 F cm^{-2}	12.1 Wh kg^{-1}	1
NHPC	182.0 F g^{-1}	71.8 Wh kg^{-1}	2
CT-SWNT-$NiCo_2O_4$	588 mF cm^{-2}	138 μWh cm^{-2}	3
meso-microporous carbons	254 F g^{-1}		4
1D-HCNB-x	370 F g^{-1}		5
balsa carbon/CNTs	1940 mF cm^{-2}		6
nitrogen-doped graphene	152.8 μF cm^{-2}	16.9 Wh kg^{-1}	7
PANI@PS/FTO	753 F g^{-1}		8
MXene-knotted CNT	130 F g^{-1}	59 Wh kg^{-1}	9
Our work	254.6 F g^{-1} in H_2SO_4	73.2 Wh kg^{-1}	

References

1. Y. Y. Chen， H. W. Hou， B. Liu， M. Y. Li， L. Chen， C. Z. Chen， S. F. Wang，Y. Y. Li， D. Y. Min. *Chem. Eng. J.* **2023**, 454, 140453.

2. Z. W. Li, Y. H. Xu, J. X. Cui, H. Dou, X. G. Zhang. *J. Power Sources* **2023**, 555, 232386.

3. Z. P. Yang, X. Y. Yang, T. T. Yang, Y. F. Cao, C. J. Zhang, Y. Y. Zhang, P. Li, J. F. Yang, Y. Y. Ma, Q. W. Li. *Energy Storage Mater*. **2023**, 54, 51-59.

4. H. B. MotejaddedEmrooz, M. S. H. Naghavi, S. Mohammadi, S. M. Mousavi-Khoshdel. *J. Energy Storage* **2022**, 56, 105989.

5. Minjun Kim, Chaohai Wang, Jacob Earnshaw, Teahoon Park, Nasim Amirilian, Aditya Ashok, Jongbeom Na, Minsu Han, Alan E. Rowan, Jiansheng Li, Jin Woo Yi, Yusuke Yamauchi. *J. Mater. Chem. A*, **2022**,10, 24056-24063.

6. Q. He, R. He, A. Zia, G. H. Gao, Y. F. Liu, M. Neupane, M. Wang, Z. Benedict, K. K. Al-Quraishi, L. Li, P. Dong, Y. C. Yang. *Small* **2022**, 50, 2200272.

7. S. Zhu, F. Zhang, H.-G. Lu, J. Sheng, L. N. Wang, S.-D. Li, G. Y. Han, Y. Li. *ACS Materials Lett*. **2022**, 4, 10, 1863–1871.

8. S. Peng, B. Liu, X. Y. Zhang, W. H. Li, S. Y. Chen, C. L. Hu, X. Q. Liu, J. Y. Liu, J. Chen. *ACS Appl. Energy Mater*. **2021**, 4, 12, 14766–14777.

9. X. Gao, X. Du, T. S. Mathis, M. M. Zhang, X. H. Wang, J. L. Shui, Y. Gogotsi, M. Xu. *Nat. Commun*. **2020**; 11: 6160.